Study of a pseudo-stationary state for a corrosion model: Existence and numerical approximation

Claire Chainais-Hillairet [a], Thomas O. Gallouët [b,c,*]

[a] *Université de Lille, Laboratoire Paul Painlevé, Cité Scientifique, 59655 Villeneuve d'Ascq Cedex, France*
[b] *Université Libre de Bruxelles (ULB), Département de mathématique, boulevard du Triomphe, 1050 Brussels, Belgium*
[c] *Project-Team MEPHYSTO, Inria Lille - Nord Europe, 59655 Villeneuve d'Ascq, France*

A B S T R A C T

In this paper, we consider a system of partial differential equations describing the pseudo-stationary state of a dense oxide layer. We investigate the question of existence of a solution to the system and we design a numerical scheme for its approximation. Numerical experiments with real-life data shows the efficiency of the method. Then, the analysis is fulfilled on a simplified model.

© 2016 Elsevier Ltd. All rights reserved.

1. Introduction

1.1. General framework of the study

The concept for long term storage of high-level radioactive waste in France under study is based on an underground repository. The waste shall be confined in a glass matrix and then placed into cylindrical steel canisters. These containers shall be placed into micro-tunnels in the highly impermeable Callovo-Oxfordian claystone layer at a depth of several hundred metres.

The long-term safety assessment of the geological repository has to take into account the degradation of the carbon steel used for the waste overpacks and the cell disposal liners, which are in contact with the claystone formation. This degradation is mainly caused by generalized corrosion processes which take place under anaerobic conditions. As a tool to investigate the corrosion processes at the surface of the carbon

steel canisters, the Diffusion Poisson Coupled Model (DPCM) for corrosion has been developed by Bataillon et al. [1].

The DPCM model describes the evolution of a dense oxide layer in the region of contact between the claystones and the metal. This is based on a coupled system of electromigration–diffusion equations for the transport of the charge carriers in the oxide layer, and a Poisson equation for the electric potential. The inter-actions between the oxide layer and the clay soil or the metal are described in terms of Robin boundary condi-tions. The system includes moving boundary equations based on the Pilling–Bedworth ratio [2]. As the oxide layer is very thin compared to the waste overpack size, the model proposed in [1] is a one-dimensional model.

The questions of existence of a solution to the full DPCM model and of long-time behaviour are still open questions, due to the complexity of the model. However, some results have been obtained for a simplified model where only two species of charge carriers (electrons and ferric cations) are taken into account and where the domain is fixed. In [3], Chainais-Hillairet and Lacroix-Violet prove the existence of an evolutive solution for this simplified model, while [4] deals with the existence of a stationary solution.

In [5], Bataillon et al. proposed a numerical method for the approximation of the DPCM model. This numerical scheme has been implemented in the simulation code CALIPSO, developed at ANDRA (the French nuclear waste management agency). The convergence of the scheme has been established by Chainais-Hillairet, Colin and Lacroix-Violet in [6] for the two-species model on a fixed domain. The long time simulations presented in [5] highlighted the existence of a pseudo stationary state: a state where all the density profiles, as the profile of the electric potential and the size of the oxide layer, are constant, while both interfaces are moving at the same velocity. Moreover, it appears that the pseudo stationary state can be reached more or less quickly depending on the value of the pH.

In many cases of application, the significant solution to the DPCM model may be the pseudo stationary one and in order to reduce the numerical costs, it is interesting to propose a scheme for its direct computation. Therefore, we propose in this paper an efficient numerical method for the approximation of the pseudo stationary state of the DPCM model. Moreover, we investigate the question of existence of a pseudo steady state on a simplified model. We also justify our choice of scheme with the study of its application to the simplified model: we will see that the scheme that we propose is exact in this case. The existence of a pseudo steady state is not so obvious and seems strongly related to the boundary conditions. Indeed, in [7–9], Aiki and Muntean consider a system of reaction–diffusion equations on a moving domain describing concrete carbonation. In this case, only one boundary is free and there is no steady-state: they prove that the thickness of the domain increases following a $\sqrt{t}$-law.

1.2. Presentation of the DPCM model

The DPCM model was introduced in [1]. It consists of three drift–diffusion equations for the densities of charge carriers – ferric cations (P), electrons (N) and oxygen vacancies (C) –, coupled with one elliptic equation for the electric potential (Ψ) and two evolutive equations for the interfaces of the domain (X_0, X_1).

We consider here the dimensionless DPCM model. We will first present the equations and then give a sense to all the parameters involved in the equations. Let us mention that the scaling in time is performed with respect to the characteristic time of the cations. The equations for the carrier densities P, N, C, as the boundary conditions, have the same form. For $U = P, N$ or C, they are written:

$$\varepsilon_U \partial_t U + \partial_x J_U = 0, \qquad J_U = -\partial_x U - z_U U \partial_x \Psi \quad \text{in } (X_0(t), X_1(t)), \forall t \geq 0, \tag{1a}$$

$$-J_U + U X_0'(t) = r_U^0(U(X_0(t)), \Psi(X_0(t))) \quad \text{on } x = X_0(t), \forall t \geq 0, \tag{1b}$$

$$J_U - U X_1'(t) = r_U^1(U(X_1(t)), \Psi(X_1(t)), V) \quad \text{on } x = X_1(t), \forall t \geq 0, \tag{1c}$$

where z_U is the charge number of the carrier and ε_U is the ratio of the mobility coefficient with respect to the mobility coefficient of the cations (due to the choice of the time scaling). For $U = P, N, C$, we have respectively $z_U = 3, -1, 2$, and $\varepsilon_U = 1, \frac{D_1}{D_2}, \frac{D_1}{D_3}$.

The functions r_U^0 and r_U^1 defining the boundary conditions in (1b), (1c) are linear and monotonically increasing with respect to their first argument. More precisely, we assume that they have the following form:

$$r_U^0(s, x) = \beta_U^0(x)s - \gamma_U^0(x), \tag{2a}$$

$$r_U^1(s, x, V) = \beta_U^1(V - x)s - \gamma_U^1(V - x), \tag{2b}$$

where $\beta_U^0, \beta_U^1, \gamma_U^0, \gamma_U^1$ are smooth positive functions defined as:

$$\gamma_P^0(x) = m_P^0 P^m e^{-3b_P^0 x} \qquad\qquad \gamma_P^1(y) = k_P^1 P^m e^{3a_P^1 y}$$

$$\beta_P^0(x) = m_P^0 e^{-3b_P^0 x} + k_P^0 e^{3a_P^0 x} \qquad \beta_P^1(y) = m_P^1 e^{-3b_P^1 y} + k_P^1 e^{3a_P^1 y}$$

$$\gamma_N^0(x) = m_N^0 e^{b_N^0 x} \qquad\qquad \gamma_N^1(y) = k_N^1 N_{metal} \log(1 + e^{-y})$$

$$\beta_N^0(x) = k_N^0 e^{-a_N^0 x} \qquad\qquad \beta_N^1(y) = m_N^1$$

$$\gamma_C^0(x) = m_C^0 e^{-2b_C^0 x} \qquad\qquad \gamma_C^1(y) = k_C^1 e^{3a_C^1 y}$$

$$\beta_C^0(x) = m_C^0 e^{-2b_C^0 x} + k_C^0 e^{2a_C^0 x} \qquad \beta_C^1(y) = m_C^1 e^{-3b_C^1 y} + k_C^1 e^{3a_C^1 y}$$

The equation on the electric potential Ψ is a Poisson equation, written as:

$$-\lambda^2 \partial_{xx}^2 \Psi = 3P - N + 2C + \rho_{hl}, \quad x \in (X_0(t), X_1(t)), \tag{3a}$$

$$\Psi - \alpha_0 \partial_x \Psi = \Delta \Psi_0^{pzc}, \quad x = X_0(t), \tag{3b}$$

$$\Psi + \alpha_1 \partial_x \Psi = V - \Delta \Psi_1^{pzc}, \quad x = X_1(t). \tag{3c}$$

The moving boundary equations are written as:

$$\frac{dX_0}{dt} = v_d^0(t) + \frac{dX_1}{dt}\left(1 - \frac{\Omega_{ox}}{m\Omega_{Fe}}\right), \tag{4a}$$

$$\frac{dX_1}{dt} = -\frac{D_3}{4D_1}\frac{\Omega_{Fe}}{\Omega_{ox}}(J_C(X_1) + C X_1'(t)), \tag{4b}$$

where $v_d^0(t)$ is the dissolution speed of the layer, given by $v_d^0(t) = k_d^0 e^{-5a_d^0 \Psi(X_0(t))}$.

The system is supplemented with initial conditions:

$$N(x, 0) = N^0(x), \qquad P(x, 0) = P^0(x), \qquad C(x, 0) = C^0(x), \quad x \in (0, 1), \tag{5a}$$

$$X_0(0) = 0, \qquad X_1(0) = 1. \tag{5b}$$

Let us now shortly explain the parameters of the model. We first introduce the physical parameters:

- D_1, D_2 and D_3 are respectively the mobility or diffusion coefficients of cations, electrons and oxygen vacancies. D_1 and D_3 have the same order of magnitude, but $D_1 \ll D_2$ due to the difference of size between cations and electrons and the resulting difference of mobilities.
- (a_U^0, b_U^0) for $U = P, N, C, r, (a_U^1, b_U^1)$ for $U = P, C$ and a_d^0 are positive transfer coefficients. They satisfy:

$$a_U^0 + b_U^0 = 1 = a_U^1 + b_U^1 \quad \text{for } U = P, N, C. \tag{6}$$

- Ω_{ox} is the molar volume of the oxide, Ω_{Fe} is the molar volume of the metal and m is the number of moles of iron per mole of oxide ($m = 3$ for magnetite). As the Pilling–Bedworth ratio is the ratio of elementary cell volume of metal oxide to the elementary cell volume of the equivalent metal where the oxide has been created, it is equal to $\Omega_{ox}/(m\Omega_{Fe})$ and it acts in (4a).

The following parameters come from physical parameters but are concerned by the scaling. There are scaled parameters:

- $(m_P^i, k_P^i)_{i=0,1}, (m_N^i, k_N^i)_{i=0,1}, (m_C^i, k_C^i)_{i=0,1}, (n_N^0, p_N^0), k_d^0$ are interface kinetic functions. We assume that these functions are constant and strictly positive.
- P^m is related to the maximum occupancy for octahedral cations in the host lattice.
- N_{metal} is related to the electron density of state in the metal (Friedel model).
- ρ_{hl} is the related to net charge density of the ionic species in the host lattice. We assume that ρ_{hl} is homogeneous.
- $\Delta\Psi_0^{pzc}, \Delta\Psi_1^{pzc}$ are related respectively to the outer and the inner voltages of zero charge.
- $\lambda^2, \alpha_0, \alpha_1$ are positive dimensionless parameters coming from the scaling.

In the system (1)–(5), V is an applied potential and the system corresponds to a "potentiostatic case". However, the system (1)–(5) can be supplemented with an additional equation ensuring the electron charge balance at the inner interface :

$$-3\left(J_P + PX_1'(t) + \frac{D_3}{4D_1}(J_C + CX_1'(t))\right) + \frac{D_2}{D_1}(J_N + NX_1'(t)) = \tilde{J}, \quad x = X_1(t). \tag{7}$$

This corresponds to a "galvanostatic case". If $\tilde{J} = 0$, we speak of free corrosion and the resulting V is called "free corrosion potential".

Remark 1.1. The DPCM model involves many parameters. Some of these parameters are known from the literature or given by physical experiments. Some other ones, as k_d^0 for instance, can be set up thanks to numerical experiments. The scaling process leading to a dimensionless system of equations is partly described in [10, Section 5].

1.3. Main results

A numerical scheme was proposed in [5] in order to compute an approximate solution to the system (1)–(5) (or (1)–(7)). This scheme is a fully implicit Euler scheme in time and a finite volume scheme in space with a Scharfetter–Gummel approximation of the convection–diffusion fluxes. The numerical experiments, see for instance Figure 6.2 in [5] or Figure 36 in [1], show the apparition in large time of a pseudo steady state. The paper is devoted to the theoretical and numerical analysis of this steady state. It is structured as follows.

In Section 2, we define the steady state and we propose a finite volume scheme, closely related to the scheme from [5], in order to compute an approximate solution. We discuss the numerical implementation (as the scheme leads to a nonlinear system of equations). We also present and analyse some numerical results obtained with real-life data.

In Section 3, we investigate the question of existence of a steady state. We perform a complete analysis on a simplified model. The existence result is stated in Theorem 3.1. Then, Section 4 is devoted to the numerical analysis of the scheme proposed in Section 2 and applied to the simplified model. We prove that the scheme is exact in this case.

2. Study of the pseudo stationary state

2.1. Characterization of the pseudo stationary state

The numerical experiments presented in [5,1] show the apparition, in large time, of a pseudo stationary state. Indeed, it appears that the thickness of the oxide layer become constant, as well as the profiles of the

densities and of the electric potential, while both interfaces are moving at the same velocity. In order to define this pseudo stationary state, we first reformulate the DPCM model (1)–(4) on a fixed domain, as in [5].

Therefore, we use the following change of variables:

$$\bigcup_{0 \le t \le T} [X_0(t), X_1(t)] \times \{t\} \to [0, 1] \times [0, T]$$

$$(x, t) \mapsto \left(\xi = \frac{x - X_0(t)}{X_1(t) - X_0(t)}, t \right).$$

We set

$$L(t) = X_1(t) - X_0(t). \tag{8}$$

Equations (1) on $U = P, N, C$ rewrite as:

$$\varepsilon_U L(t) \partial_t (L(t)U) + \partial_\xi \hat{J}_U = 0, \tag{9a}$$

$$\hat{J}_U = -\partial_\xi U - [z_U \partial_\xi \Psi + \varepsilon_U L(t) (X_0'(t) + \xi L'(t))] U, \quad \xi \in (0, 1), \tag{9b}$$

$$-\hat{J}_U = L(t) r_U^0(U, \Psi), \quad \xi = 0, \tag{9c}$$

$$\hat{J}_U = L(t) r_U^1(U, \Psi, V), \quad \xi = 1. \tag{9d}$$

Equations (3) on Ψ rewrite as:

$$-\frac{\lambda^2}{L(t)^2} \partial_{\xi\xi}^2 \Psi = 3P - N + 2C + \rho_{hl}, \quad \xi \in (0, 1), \tag{10a}$$

$$\Psi - \frac{\alpha_0}{L(t)} \partial_\xi \Psi = \Delta \Psi_0^{pzc}, \quad \xi = 0, \tag{10b}$$

$$\Psi + \frac{\alpha_1}{L(t)} \partial_\xi \Psi = V - \Delta \Psi_1^{pzc}, \quad \xi = 1. \tag{10c}$$

Let us denote $\Pi = \frac{\Omega_{ox}}{m \Omega_{Fe}}$ and $K = \frac{D_3}{4D_1} \frac{\Omega_{Fe}}{\Omega_{ox}}$. Then, the moving boundary equations rewrite as:

$$\frac{dX_0}{dt} = v_d^0(t) + \frac{dX_1}{dt}(1 - \Pi), \tag{11a}$$

$$\frac{dX_1}{dt} = -K r_C^1(C(1, t), \Psi(1, t), V), \tag{11b}$$

$$\text{with } v_d^0(t) = k_d^0 e^{-5a_d^0 \Psi(0, t)}. \tag{11c}$$

Moreover, in the galvanostatic case, the additional equation becomes

$$-3 \left(\hat{J}_P + \frac{\varepsilon_C}{4} \hat{J}_C \right) + \varepsilon_N \hat{J}_N = \tilde{J}, \quad \xi = 1. \tag{12}$$

We are now able to write the set of equations which will define the steady state model for DPCM. The unknowns of this model are the densities of charge carriers P, N, C, the electric potential Ψ, the velocity of the interfaces δ and the thickness of the oxide layer ℓ. The set of equations is obtained from (9)–(11) by letting down the dependency with respect to time and by setting $L(t) = \ell$ and $X_0'(t) = X_1'(t) = \delta$. It writes as:

- Equations and boundary conditions for $U = P, N, C$:

$$\partial_\xi \hat{J}_U = 0, \qquad \hat{J}_U = -\partial_\xi U - (z_U \partial_\xi \Psi + \varepsilon_U \ell \delta)U, \quad \xi \in (0, 1), \tag{13a}$$

$$-\hat{J}_U = \ell r_U^0(U, \Psi), \quad \xi = 0, \tag{13b}$$

$$\hat{J}_U = \ell r_U^1(U, \Psi, V), \quad \xi = 1. \tag{13c}$$

- Equation and boundary conditions for Ψ:

$$-\frac{\lambda^2}{\ell^2}\partial^2_{\xi\xi}\Psi = 3P - N + 2C + \rho_{hl}, \quad \xi \in (0,1), \tag{14a}$$

$$\Psi - \frac{\alpha_0}{\ell}\partial_\xi\Psi = \Delta\Psi_0^{pzc}, \quad \xi = 0, \tag{14b}$$

$$\Psi + \frac{\alpha_1}{\ell}\partial_\xi\Psi = V - \Delta\Psi_1^{pzc}, \quad \xi = 1. \tag{14c}$$

- Equation for the velocity δ and the thickness ℓ:

$$\delta = \frac{v_d^0}{\Pi}, \tag{15a}$$

$$\ell = -K\frac{\hat{J}_C(1)}{\delta}, \tag{15b}$$

$$\text{with } v_d^0 = k_d^0 e^{-5a_d^0\Psi(0)}. \tag{15c}$$

The set of equations (13)–(15) describing the steady state will be denoted ($\mathbf{M}$) in the sequel. It describes the potentiostatic case. In the galvanostatic case, V is defined by an additional equation:

$$-3\left(\hat{J}_P + \frac{\varepsilon_C}{4}\hat{J}_C\right) + \varepsilon_N\hat{J}_N = 0. \tag{16}$$

The system (13)–(16) will be denoted ($\mathbf{Mg}$).

2.2. Numerical scheme

In order to compute an approximate solution to ($\mathbf{M}$) or ($\mathbf{Mg}$), we propose a finite volume scheme close to the one introduced in [5]. Therefore, we consider a mesh for the domain $[0,1]$, which is not necessarily uniform, *i.e* a family of given points $(x_i)_{0\le i\le I+1}$ satisfying

$$x_0 = 0 < x_1 < x_2 < \cdots < x_I < x_{I+1} = 1.$$

Then, for $1 \le i \le I-1$, we define $x_{i+\frac{1}{2}} = \frac{x_i+x_{i+1}}{2}$ and we set $x_{\frac{1}{2}} = x_0 = 0, x_{I+\frac{1}{2}} = x_{I+1} = 1$. The cells of the mesh are the intervals $(x_{i-\frac{1}{2}}, x_{i+\frac{1}{2}})$ for $1 \le i \le I$. Let us set

$$h_i = x_{i+\frac{1}{2}} - x_{i-\frac{1}{2}}, \quad \text{for } 1 \le i \le I,$$
$$h_{i+\frac{1}{2}} = x_{i+1} - x_i, \quad \text{for } 0 \le i \le I$$

and $h = \max\{h_i, \ 1 \le i \le I\}$ is the size of the mesh.

The unknowns of the scheme for ($\mathbf{M}$) are the densities $(N_i, P_i, C_i)_{0\le i\le I+1}$ and the electric potential $(\Psi_i)_{0\le i\le I+1}$, the velocity of the interfaces δ^h and the thickness of the domain ℓ^h.

The scheme writes as:

- Scheme for Ψ:

$$-\frac{\lambda^2}{\ell^{h2}}(d\Psi_{i+\frac{1}{2}} - d\Psi_{i-\frac{1}{2}}) = h_i(3P_i - N_i + 2C_i + \rho_{hl}), \quad 1 \le i \le I, \tag{17a}$$

$$\text{with } d\Psi_{i+\frac{1}{2}} = \frac{\Psi_{i+1} - \Psi_i}{h_{i+\frac{1}{2}}}, \quad 0 \le i \le I, \tag{17b}$$

$$\Psi_0 - \frac{\alpha_0}{\ell^h}d\Psi_{\frac{1}{2}} = \Delta\Psi_0^{pzc}, \tag{17c}$$

$$\Psi_{I+1} + \frac{\alpha_1}{\ell^h}d\Psi_{I+\frac{1}{2}} = V - \Delta\Psi_1^{pzc}. \tag{17d}$$

• Scheme for $U = P, N, C$:

$$\mathcal{G}_{U,i+\frac{1}{2}} - \mathcal{G}_{U,i-\frac{1}{2}} = 0, \quad 0 \leq i \leq I, \tag{18a}$$

$$\mathcal{G}_{U,i+\frac{1}{2}} = \frac{1}{h_{i+\frac{1}{2}}} \left(B\Big(h_{i+\frac{1}{2}}\big(z_U d\Psi_{i+\frac{1}{2}} + \varepsilon_U \ell^h \delta^h\big)\Big)U_i \right. \tag{18b}$$

$$\left. - B\Big(-h_{i+\frac{1}{2}}\big(z_U d\Psi_{i+\frac{1}{2}} + \varepsilon_U \ell^h \delta^h\big)\Big)U_{i+1} \right), \quad 1 \leq i \leq I, \tag{18c}$$

$$-\mathcal{G}_{U,\frac{1}{2}} = \ell^h r_U^0(U_0, \Psi_0), \tag{18d}$$

$$\mathcal{G}_{U,I+\frac{1}{2}} = \ell^h r_U^1(U_{I+1}, \Psi_{I+1}), \tag{18e}$$

where B is given by the Bernoulli function

$$B(x) = \frac{x}{e^x - 1} \quad \forall x \neq 0, \ B(0) = 1. \tag{19}$$

• Scheme for δ and ℓ:

$$\delta^h = \frac{k_d^0}{\Pi} e^{-5a_d^0 \Psi_0}, \tag{20a}$$

$$\ell^h = -K \frac{\mathcal{G}_{C,I+\frac{1}{2}}}{\delta^h}. \tag{20b}$$

The scheme (17)–(20) will be denoted by (**S**). In the galvanostatic case, we have to discretized the additional equation (16). We write:

$$-3\left(\mathcal{G}_{P,I+\frac{1}{2}} + \frac{\varepsilon_C}{4}\mathcal{G}_{C,I+\frac{1}{2}}\right) + \varepsilon_N \mathcal{G}_{N,I+\frac{1}{2}} = 0. \tag{21}$$

It adds one unknown and one nonlinear equation to the previous system of nonlinear equations (**S**). In the sequel, we will denote this scheme (**Sg**).

Let us remark that the choice of the Bernoulli function for B corresponds to a Scharfetter–Gummel approximation of the convection–diffusion fluxes. These numerical fluxes have been introduced by Il'in in [11] and Scharfetter and Gummel in [12] for the numerical approximation of linear the drift–diffusion system arising in semiconductor modelling. It has been established by Lazarov, Mishev and Vassilevski in [13] that they are second-order accurate in space. Dissipativity of the Scharfetter–Gummel scheme with a backward Euler time discretization for the classical drift–diffusion system was proved in [14] and Chatard in [15]. One crucial property of the Scharfetter–Gummel fluxes is that they generally preserve steady-states. We will see in Section 4 that this property remains true in our case.

2.3. Implementation and numerical results

2.3.1. Implementation

The scheme (**S**) can be seen as the limit $\Delta t \to +\infty$ of the scheme proposed in [5] (in this paper, the system is the evolutive DPCM model and Δt is the time step of the scheme). Therefore, the implementation is similar to the one proposed in [5]. The main difference is that the equations for the moving boundary interfaces, written on X_0 and X_1 in the evolutive case, become equations on the velocity δ^h and the thickness ℓ^h.
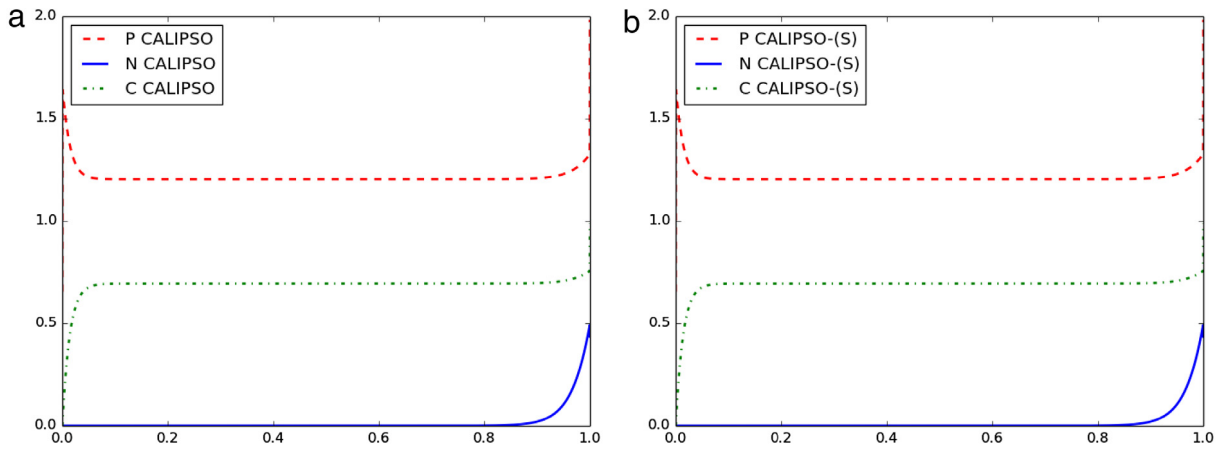
Fig. 2.1. Potentiostatic case with $V = 0.5$, at pH $= 9.3$. Density profiles at the steady-state, (a) reached by the code CALIPSO for the evolutive system, (b) directly computed by CALIPSO-(S).

The scheme (**S**) leads to a nonlinear system of equations $F(Z) = 0$, whose unknown vector is

$$Z = ((\Psi_i, P_i, N_i, C_i)_{0 \leq i \leq I+1}, \delta^h, \ell^h) \in \mathbb{R}^{4(I+2)+2}$$

in the potentiostatic case or $Z = ((\Psi_i, P_i, N_i, C_i)_{0 \leq i \leq I+1}, \delta^h, \ell^h, V) \in \mathbb{R}^{4(I+2)+3}$ in the galvanostatic case. A Newton's method is used to solve the nonlinear system of equations, with a Schur complement technique for the solution of linear systems. We refer to [5] for more details. The implementation of the scheme (**S**) has been done in the code CALIPSO and we will denote from now on CALIPSO-(S) this part of the code.

One difficult task is the choice of the initialization for the Newton's method. We can start with a set of values for $((P_i), (N_i), (C_i))_{0 \leq i \leq I}$ given in the input data file and compute $(\Psi_i)_{0 \leq i \leq I+1}$ as a solution to (17). In this case, we choose some constant values for the densities and the convergence of the Newton's method is not always ensured. In practice, it works only for very few values of the pH. With the set of parameters given in the Appendix, it works for instance for pH $= 9.3$.

Then, an other strategy is to apply a continuation process : we start with a pH value that is supporting the first method and we use the computed solution as initial data for a new value of pH, close to the preceding one. Thus, using small increments for the value of the pH, we are able to compute the pseudo stationary state for any value of the pH, in the potentiostatic as in the galvanostatic case.

2.3.2. Numerical experiments

Qualitative results.

We first want to compare the different profiles computed with the code CALIPSO for the evolutive system at a large time and the pseudo steady state directly computed with the code CALIPSO-(S). In practice, we consider that the steady state is reached by the evolutive scheme when the relative variation of the thickness of the oxide layer is small with respect to a given parameter named ϵ_{tol}. This parameter must be sufficiently small in order to obtain accurate results. In practice, we choose $\epsilon_{tol} = 10^{-6}$.

The set of parameters defining the test case is given in the Appendix. We choose a Chebychev mesh (so that the mesh is refined at the boundaries, see [5]) with 2000 cells. In the evolutive case, the time step is $\Delta t = 1000$ s (before scaling).

Figs. 2.1 and 2.2 show the profiles of the densities and of the electric potential in the potentiostatic case with $V = 0.5$ and pH $= 9.3$. We observe that the profiles computed with the evolutive scheme and with (**S**) are similar. The conclusion is the same in the galvanostatic case with pH $= 9.3$, see Figs. 2.3 and 2.4.
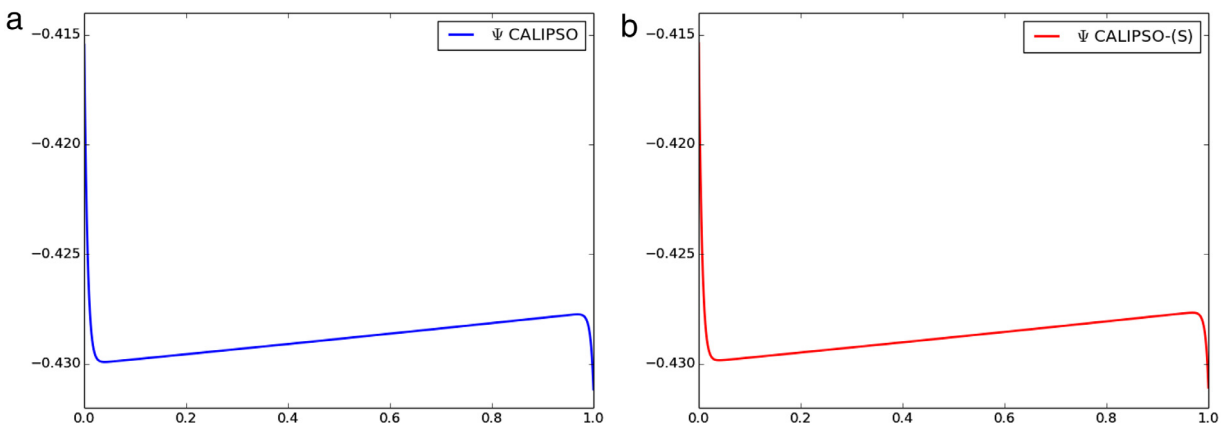
*Efficiency of the direct computation with (**S**) or (**Sg**)*
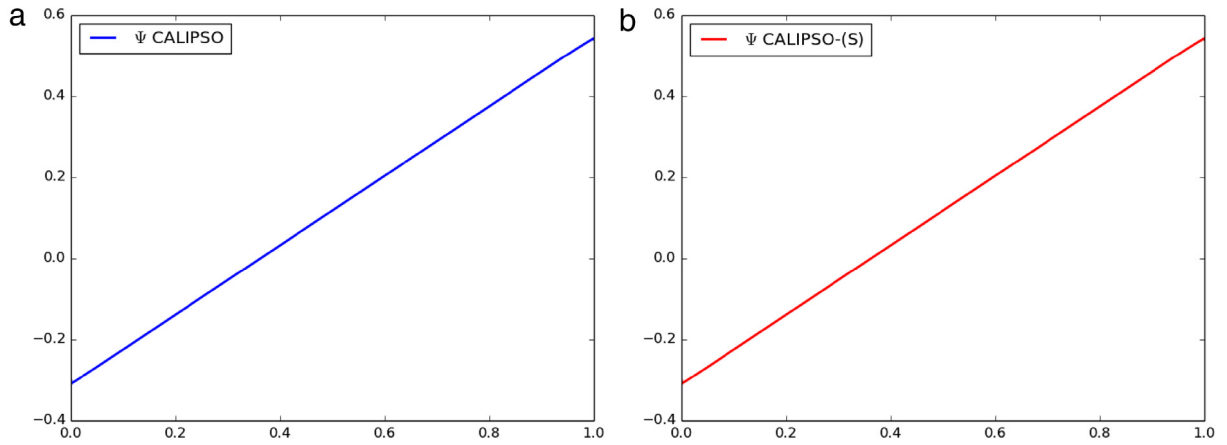
Fig. 2.2. Potentiostatic case with $V = 0.5$, at pH $= 9.3$. Profile of the electric potential at the steady-state, (a) reached by the code CALIPSO for the evolutive system, (b) directly computed by CALIPSO-(S).
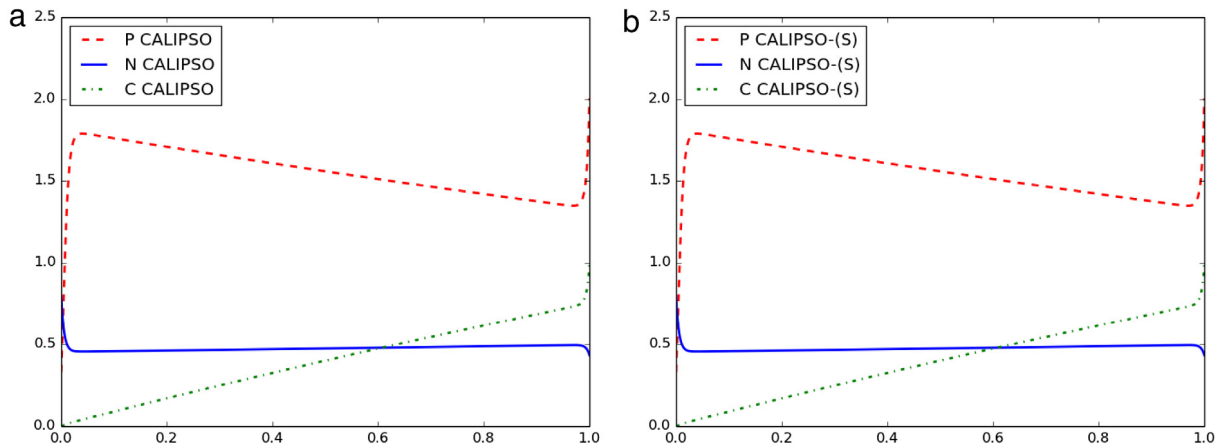
Fig. 2.3. Galvanostatic case at pH $= 9.3$. Density profiles at the steady-state, (a) reached by the code CALIPSO for the evolutive system, (b) directly computed by CALIPSO-(S).

Fig. 2.4. Galvanostatic case at pH $= 9.3$. Profile of the electric potential at the steady-state, (a) reached by the code CALIPSO for the evolutive system, (b) directly computed by CALIPSO-(S).
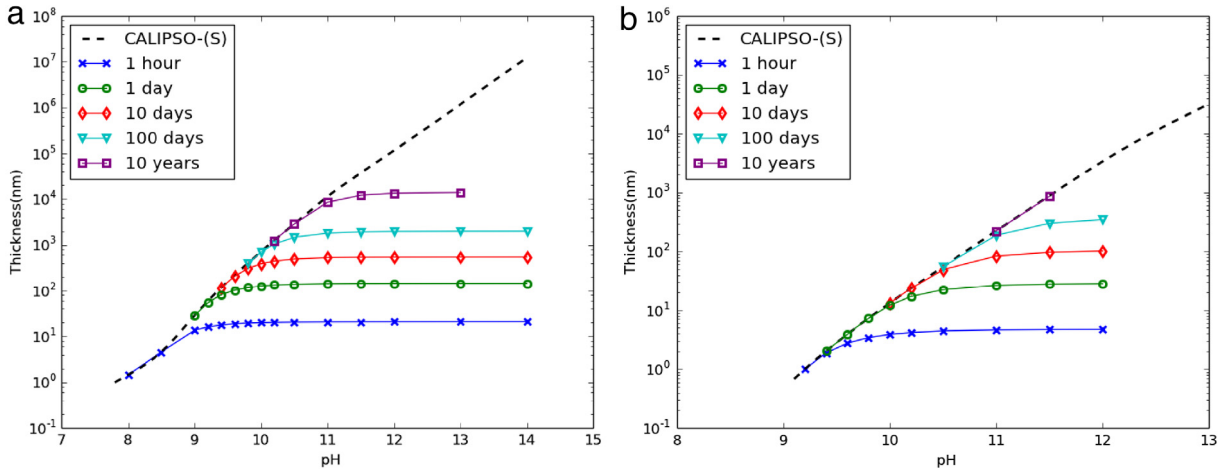
Table 2.1
Number of Newton iterations.

	Potentiostatic case		Galvanostatic case	
	pH = 9.3	pH = 10.2	pH = 9.3	pH = 10.2
CALIPSO-(S)	12	57	23	68
CALIPSO	2359	12,037	97	3654

Fig. 2.5. Dependency of the thickness of the oxide layer with respect to the pH value. Reached by CALIPSO-(S) and CALIPSO for increasing final time, (a) potentiostatic case, (b) galvanostatic case.

We now compare the codes CALIPSO and CALIPSO-(S) in term of the number of iterations of the Newton's method. Indeed, as the scheme for the evolutive DPCM model implemented in the code CALIPSO is a fully implicit scheme, the discrete solution at each time step is computed with a Newton's method. In this case, the values for the initialization of the method are given by the solution at the preceding time step.

In Table 2.1, we present the number of iterations of the Newton's method necessary for the computation of the steady state with CALIPSO and CALIPSO-(S) for two values of pH. At pH = 9.3, we can initialize the Newton's method in CALIPSO-(S) with a constant set of discrete densities. But, the solution at pH = 10.2 is obtained thanks to the continuation process described above: starting from pH = 9.3 and increasing the value of pH up to 10.2 by increments of pH equal to 10^{-2}. The stopping criterion in both codes are the same and equal to $\epsilon_{Newt} = 10^{-8}$. Table 2.1 shows the efficiency of the direct computation of the steady state with (**S**) or (**Sg**).

Fig. 2.5 shows the dependency of the thickness of the oxide layer with respect to the pH value. We remark that the pseudo steady state is reached earlier for low values of the pH (close to 9) than for high values. Therefore, the computation of the steady state with CALIPSO-(S) is the more useful than the pH is high.

*Sensitivity of the models (**M**) and (**Mg**) to the parameters.*

The thickness of the oxide layer at the steady state strongly depends on the pH and, in the potentiostatic case, on the applied potential V. We can already see on Fig. 2.5 that the steady state thickness follows a logarithmic law with respect to pH with a slope equal to 1. It is related to the fact that k_d^0 is proportional to 10^{-pH}. The depassivation pH is defined as the supremum of the pH values for which the thickness of the corrosion layer is smaller the 1nm.

Fig. 2.6 shows that the depassivation pH highly depends on the value of k_d^0 and therefore the importance of giving a very good approximation of this data. The slope of the logarithmic law does not change. The value of $k_{d,ref}^0$ is given in the Appendix. The dependence on the parameter V, in the potentiostatic case, is showed in Fig. 2.7.
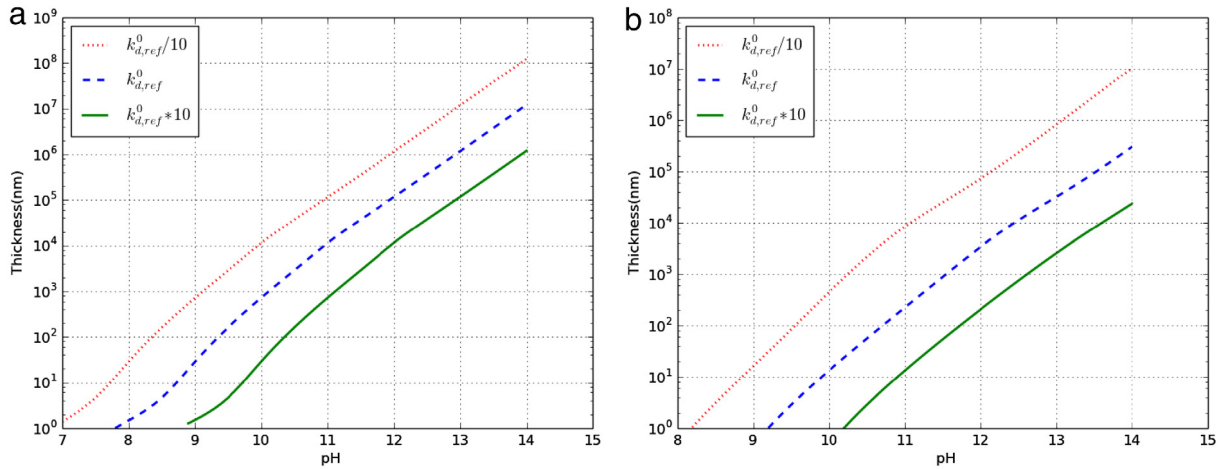
Fig. 2.6. Dependency of the thickness of the oxide layer with respect to the pH value. Reached by CALIPSO-(S) for multiple values of k_d^0. (a) potentiostatic case, (b) galvanostatic case.
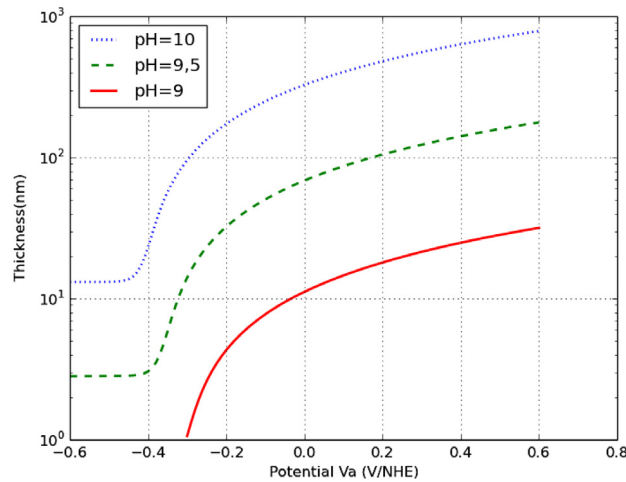

Fig. 2.7. Dependency of the thickness of the oxide layer with respect to the applied potential V. Reached by CALIPSO-(S) for multiple values of the pH in the potentiostatic case.

3. Mathematical study of a simplified model

The existence of a solution to the evolutive DPCM model (1)–(5) is an open question. The main difficulties are of three types: the system is strongly coupled (the coupling arises in the equations and in the boundary conditions), the boundary conditions are Robin boundary conditions and the interfaces are moving. In [3], Chainais-Hillairet and Lacroix-Violet prove the existence of a solution in a simplified case where only electrons and cations are taken into account and therefore the domain is fixed. Convergence of backward Euler scheme in time and finite volume scheme in space for the same simplified system has been established in [6]. Chainais-Hillairet and Lacroix-Violet have also proved in [4] the existence of a steady state for the two species system on a fixed domain, while the convergence of a finite volume scheme is studied in [10].

In this paper, we have introduced the system defining the steady state of the full DPCM model: (**M**) in the potentiostatic case and (**Mg**) in the galvanostatic case. From now on, we will focus on the potentiostatic
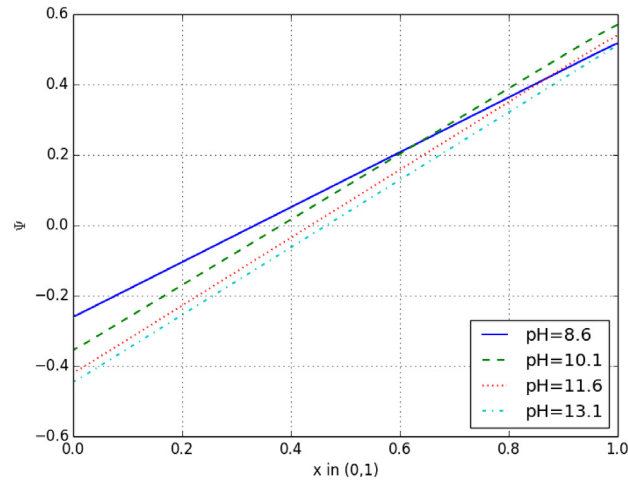
Fig. 3.1. Profiles of the electric potential for different values of pH in the potentiostatic case.

case. The coupling is still strong. However, the numerical experiments done for (**M**) show, for different values of the pH, that the electric potential Ψ has a linear profile, see Fig. 3.1.

This observation leads us to the following simplification in (**M**): we cancel the right-hand-side in the Poisson equation on Ψ (14). Therefore Ψ is effectively an affine function on $[0,1]$ which is explicitly determined, but the densities and the electric potential are still coupled *via* the boundary conditions in the equations for the densities. This simplified model can be seen as a toy model for the theoretical analysis and the numerical analysis. We will denote it (**TM**).

In this section, after introducing (**TM**), we prove the existence of a solution. The question of the positivity of the densities and of the thickness of the oxide layer is also investigated. The numerical analysis of the schemes deduced from (**S**) for (**TM**) is proposed in Section 4.

3.1. Presentation of the toy model

The simplified model (**TM**) is obtained by cancelling the right hand side of the equation on Ψ (14). It is given by the following set of equations:

- Equation and boundary conditions for Ψ:

$$-\frac{\lambda^2}{\ell^2}\partial_{\xi\xi}^2 \Psi = 0, \quad \xi \in (0,1), \tag{22a}$$

$$\Psi - \frac{\alpha_0}{\ell}\partial_\xi \Psi = \Delta \Psi_0^{pzc}, \quad \xi = 0, \tag{22b}$$

$$\Psi + \frac{\alpha_1}{\ell}\partial_\xi \Psi = V - \Delta \Psi_1^{pzc}, \quad \xi = 1. \tag{22c}$$

- Equation and boundary conditions for C

$$\partial_\xi \hat{J}_C = 0, \qquad \hat{J}_C = -\partial_\xi C - (z_C \partial_\xi \Psi + \varepsilon_C \ell \delta C), \quad \xi \in (0,1), \tag{23a}$$

$$-\hat{J}_C = \ell r_C^0(C, \Psi(0)), \quad \xi = 0, \tag{23b}$$

$$\hat{J}_C = \ell r_C^1(C, \Psi(1), V), \quad \xi = 1. \tag{23c}$$

- Equation for the velocity δ and the thickness ℓ:

$$\delta = \frac{k_d^0 e^{-5a_d^0 \Psi(0)}}{\Pi}, \tag{24a}$$

$$\ell = -K \frac{\hat{J}_C(1)}{\delta}. \tag{24b}$$

- Equation and boundary conditions for $U = P, N$.

$$\partial_\xi \hat{J}_U = 0, \qquad \hat{J}_U = -\partial_\xi U - (z_U \partial_\xi \Psi + \varepsilon_U \ell \delta U), \quad \xi \in (0,1), \tag{25a}$$

$$-\hat{J}_U = \ell r_U^0(U, \Psi(0)), \quad \xi = 0, \tag{25b}$$

$$\hat{J}_U = \ell r_U^1(U, \Psi(1), V), \quad \xi = 1. \tag{25c}$$

The computation of N and P, solutions to (25), is decoupled from (22)–(24). Therefore, the model (**TM**)corresponds to (22)–(24).

Remark 3.1. We expect the densities $U = P, N, C$ to be nonnegative and bounded. According to (24b) the flux $\hat{J}_C$ must be nonnegative. In regards of numerical results, it can be relevant to ask for $\hat{J}_P$ and $\hat{J}_N$ to be nonpositive.

3.2. Existence of a solution for (**TM**)

In order to prove the existence of a solution for (**TM**), we start with a given $\ell > 0$ and study the system (22), (23), (24a), see Lemma 3.1. Afterwards, we will prove the existence of ℓ satisfying (24b) thanks to an intermediate value theorem.

Lemma 3.1. Let $\ell > 0$. There exists a unique solution $(\Psi, C, \delta) \in (C^\infty[0,1])^2 \times \mathbb{R}_+^*$ to the system (22)–(23)–(24a).

Proof. Given $\ell > 0$, we compute Ψ solution to (22). We have:

$$\Psi(\xi) = (\Psi(1) - \Psi(0))\,\xi + \Psi(0),$$
$$\Psi(0) = \frac{(\ell + \alpha_1)\,\Delta\Psi_0^{pzc} + \alpha_0\,(V - \Delta\Psi_1^{pzc})}{\ell + \alpha_0 + \alpha_1}, \tag{26}$$
$$\Psi(1) = \frac{\alpha_1 \Delta\Psi_0^{pzc} + (\ell + \alpha_0)\,(V - \Delta\Psi_1^{pzc})}{\ell + \alpha_0 + \alpha_1}.$$

As $\max(\Delta\Psi_0^{pzc}, V - \Delta\Psi_1^{pzc})$ and $\min(\Delta\Psi_0^{pzc}, V - \Delta\Psi_1^{pzc})$ are sur- and sub-solutions of (22), Ψ is bounded independently of ℓ:

$$\min(\Delta\Psi_0^{pzc}, V - \Delta\Psi_1^{pzc}) \le \Psi(\xi) \le \max(\Delta\Psi_0^{pzc}, V - \Delta\Psi_1^{pzc}), \quad \forall \xi \in (0,1). \tag{27}$$

According to formula (26), we remark that the solution to (22) tends to a constant function when ℓ tends to 0, the constant is

$$\widetilde{\Psi} = \frac{\alpha_1 \Delta\Psi_0^{pzc} + \alpha_0(V - \Delta\Psi_1^{pzc})}{\alpha_0 + \alpha_1}.$$

When Ψ is defined, we can deduce δ:

$$\delta = \frac{k_d^0}{\Pi} e^{-5a_d^0 \Psi(0)} > 0. \tag{28}$$

Then, knowing ℓ, Ψ and δ, it is now possible to compute C solution to (23) (and similarly P and N solutions to (25)). Therefore, we use the Slotboom's change of variables, which is classical for drift–diffusion equations,

see for instance [16]. Defining $u(\xi) = U(\xi)e^{z_U\,\Psi(\xi)+\varepsilon_U\,\ell\delta\xi}$ for $U = C$ or $U = P, N$ we can rewrite (23) and (25) as:

$$\partial_\xi \hat{J}_U = 0, \qquad \hat{J}_U = -e^{-z_U\,\Psi(\xi)-\varepsilon_U\ell\delta\xi}\partial_\xi u, \quad \xi \in (0,1), \tag{29a}$$

$$\partial_\xi u - \ell\beta_U^0(\Psi(0))u = -\ell\gamma_U^0(\Psi(0))e^{z_U\,\Psi(0)}, \quad \xi = 0, \tag{29b}$$

$$\partial_\xi u + \ell\beta_U^1(V - \Psi(1))u = \ell\gamma_U^1(V - \Psi(1))e^{z_U\,\Psi(1)+\varepsilon_U\ell\delta}, \quad \xi = 1, \tag{29c}$$

Let us set $B_U^0 = \beta_U^0(\Psi(0)), B_U^1 = \beta_U^1(V - \Psi(1)), \Gamma_U^0 = \gamma_U^0(\Psi(0))$ and $\Gamma_U^1 = \gamma_U^1(V - \Psi(1))$. It is possible to give an explicit formulation of the solution to (29). The calculations have been detailed in [4, see Proposition 1]. We get:

$$u(\xi) = u(0) - \hat{J}_U \int_0^\xi e^{z_U\,\Psi(\zeta)+\varepsilon_U\,\ell\delta\zeta}d\zeta, \tag{30a}$$

$$-\hat{J}_U = \frac{\Gamma_U^1 e^{z_U\,\Psi(1)+\varepsilon_U\,\ell\delta}/B_U^1 - \Gamma_U^0 e^{z_U\,\Psi(0)}/B_U^0}{e^{z_U\,\Psi(0)}/(\ell B_U^0) + e^{z_U\,\Psi(1)+\varepsilon_U\,\ell\delta}/(\ell B_U^1) + \int_0^1 e^{z_U\,\Psi(\zeta)+\varepsilon_U\,\ell\delta\zeta}d\zeta}, \tag{30b}$$

$$u(0) = \Gamma_U^0 e^{z_U\,\Psi(0)}/B_U^0 - \hat{J}_U e^{z_U\,\Psi(0)}/(\ell B_U^0). \tag{30c}$$

Then, U is uniquely defined by $U(\xi) = u(\xi)e^{-z_U\,\Psi(\xi)-\varepsilon_U\ell\delta\xi}$ for $U = C, P, N$. It concludes the proof of Lemma 3.1. $\square$

Let us introduce $d(\ell) = \frac{z_C}{\delta}\frac{V - \Delta\Psi_1^{pzc} - \Delta\Psi_0^{pzc}}{\ell + \alpha_0 + \alpha_1}$, such that

$$z_C(\Psi(1) - \Psi(0)) = d(\ell)\ell\delta \quad \text{and} \quad e^{z_C\,\Psi(\zeta)} = e^{z_C\,\Psi(0)}e^{d(\ell)\ell\delta\zeta} \quad \forall\zeta \in [0,1].$$

It permits to rewrite (30a) and (30b) as

$$c(\xi) = c(0) - \frac{\hat{J}_C}{\ell\delta}\frac{e^{(d(\ell)+\varepsilon_C)\ell\delta\xi} - 1}{d(\ell) + \varepsilon_C}e^{z_C\,\Psi(0)}, \tag{31a}$$

$$-\frac{\hat{J}_C}{\ell\delta} = \frac{\Gamma_C^1 e^{(d(\ell)+\varepsilon_C)\ell\delta}/B_C^1 - \Gamma_C^0/B_C^0}{\delta/B_C^0 + \delta e^{(d(\ell)+\varepsilon_C)\ell\delta}/B_C^1 + \left[e^{(d(\ell)+\varepsilon_C)\ell\delta} - 1\right]/[d(\ell) + \varepsilon_C]}. \tag{31b}$$

We are now able to give the existence theorem for (**TM**).

Theorem 3.1. *Let*

$$\tilde{K}_1 = \Pi\left(K\gamma_C^1(\Delta\Psi_1^{pzc}) - \frac{\beta_C^1(\Delta\Psi_1^{pzc})}{\varepsilon_C}\right)e^{5a_d^0\tilde{\Psi}},$$

$$\tilde{K}_2 = \Pi K\frac{\beta_C^0(\tilde{\Psi})\gamma_C^1(V - \tilde{\Psi}) - \beta_C^1(V - \tilde{\Psi})\gamma_C^0(\tilde{\Psi})}{\beta_C^0(\tilde{\Psi}) + \beta_C^1(V - \tilde{\Psi})}e^{5a_d^1\tilde{\Psi}},$$

$$\tilde{C} = 1 + \frac{1}{\Pi K}\frac{k_d^0 e^{-5a_d^0\min(\Delta\Psi_0^{pzc},V - \Delta\Psi_1^{pzc})}}{m_C^0 e^{-2b_C^0\max(\Delta\Psi_0^{pzc},V - \Delta\Psi_1^{pzc})} + k_C^0 e^{2a_C^0\min(\Delta\Psi_0^{pzc},V - \Delta\Psi_1^{pzc})}}.$$

We assume

$$\min\left(\tilde{K}_1, \tilde{K}_2\right) < k_d^0 < \max\left(\tilde{K}_1, \tilde{K}_2\right). \tag{32}$$

Then, the problem (**TM**) *has a solution* $(\Psi_s, C_s, \ell_s, \delta_s) \in (C^\infty([0,1],\mathbb{R}))^2 \times (\mathbb{R}_+^*)^2$ *which satisfies* $0 \le C_s(\xi) \le \tilde{C}$ *for all* $\xi \in [0,1]$.

Proof. For a given ℓ, we will now denote by $(\Psi_\ell, C_\ell, \delta_\ell)$ the solution to (22)–(23)–(24a) given by Lemma 3.1. We introduce the function:

$$F: \ \mathbb{R}_+^* \to \mathbb{R}$$

$$\ell \mapsto -K\frac{\hat{J}_{C_\ell}}{\ell\delta_\ell}.$$

The function F is well defined and continuous. In order to prove the existence of $\ell_s > 0$ such that $F(\ell_s) = 1$, we will apply the intermediate value theorem. Therefore, we have to study the limits of F when ℓ tends to 0 and when ℓ tends to $+\infty$.

When $\ell \to +\infty$, we have the following limits :

$$\Psi_\ell(0) \to \Delta\Psi_0^{pzc}, \qquad \Psi_\ell(1) \to (V - \Delta\Psi_1^{pzc}),$$
$$d(\ell)\ell\delta_\ell \to z_C(V - \Delta\Psi_1^{pzc} - \Delta\Psi_0^{pzc}),$$
$$\delta_\ell \to \frac{k_d^0}{\Pi}e^{-5a_d^0\Delta\Psi_0^{pzc}}, d(\ell) \to 0.$$

Then, using (31b), we deduce:

$$\lim_{\ell\to+\infty} F(\ell) = K\Pi \frac{\varepsilon_C\gamma_C^1(\Delta\Psi_1^{pzc})}{\varepsilon_C k_d^0 e^{-5a_d^0\Delta\Psi_0^{pzc}} + \Pi\beta_C^1(\Delta\Psi_1^{pzc})}.$$

When $\ell \to 0$, the limits are:

$$\Psi_\ell(0) \to \widetilde{\Psi}, \qquad \Psi_\ell(1) \to \widetilde{\Psi},$$
$$d(\ell)\ell\delta_\ell \to 0, \qquad \delta_\ell \to \frac{k_d^0}{\Pi}e^{-5a_d^0\widetilde{\Psi}}.$$

Therefore,

$$\lim_{\ell\to 0} F(\ell) = K\Pi \frac{\gamma_C^1(V - \widetilde{\Psi})\beta_C^0(\widetilde{\Psi}) - \gamma_C^0(\widetilde{\Psi})\beta_C^1(V - \widetilde{\Psi})}{k_d^0 e^{-5a_d^0\widetilde{\Psi}}(\beta_C^1(V - \widetilde{\Psi}) + \beta_C^0(\widetilde{\Psi}))}.$$

Then we can see that, if $\min\left(\tilde{K}_1, \tilde{K}_2\right) < k_d^0 < \max\left(\tilde{K}_1, \tilde{K}_2\right)$,

$$\min\left(\lim_{\ell\to 0} F(\ell), \lim_{\ell\to+\infty} F(\ell)\right) < 1 < \max\left(\lim_{\ell\to 0} F(\ell), \lim_{\ell\to+\infty} F(\ell)\right).$$

It ensures the existence of ℓ_s satisfying $F(\ell_s) = 1$. Denoting by (Ψ_s, C_s, δ_s) the corresponding solution to (22)–(23)–(24a), we obtain that $(\ell_s, \Psi_s, C_s, \delta_s)$ is a solution to (**TM**).

Let us now prove that C_s is a positive, bounded function. Writing (30c) for $u = c_s$ while replacing $\hat{J}_C$ by $-\ell_s\delta_s/K$, we obtain that $c_s(0)$ is a sum of positive terms, so that it is positive. Then, writing (31a) for $c = c_s$ and $\xi = 1$, we also get that $c_s(1)$ is positive. Therefore, as c_s is a monotone function thanks to (31a), we conclude that c_s and C_s are positive in $[0, 1]$.

From (29) written for $U = C_s$ and using the known values of δ and $\hat{J}_C/(\ell\delta)$ at the steady state, we can deduce simple expressions for the boundary values of C_s:

$$\begin{cases} C_s(0) = \dfrac{1}{\beta_C^0(\Psi_s(0))} & \left(\gamma_C^0(\Psi_s(0)) + \dfrac{k_d^0 e^{-5a_d^0\Psi_s(0)}}{\Pi K}\right), \\[3mm] C_s(1) = \dfrac{1}{\beta_C^1(V - \Psi_s(1))} & \left(\gamma_C^1(V - \Psi_s(1)) - \dfrac{k_d^0 e^{-5a_d^0\Psi_s(0)}}{\Pi K}\right). \end{cases}$$

It leads, using (27) and the definition of the functions $\beta_C^0, \beta_C^1, \gamma_C^0, \gamma_C^1$,

$$C_s(0) \leq \frac{\gamma_C^0(\Psi_s(0))}{\beta_C^0(\Psi_s(0))} + \frac{k_d^0 e^{-5a_d^0\Psi_s(0)}}{\beta_C^0(\Psi_s(0))\Pi K} \leq 1 + \frac{1}{\Pi K}\frac{k_d^0 e^{-5a_d^0\Psi_s(0)}}{m_C^0 e^{-2b_C^0\Psi_s(0)} + k_C^0 e^{2a_C^0\Psi_s(0)}} \leq \tilde{C},$$

$$C_s(1) \leq \frac{\gamma_C^1(V - \Psi_s(1))}{\beta_C^1(V - \Psi_s(1))} \leq \frac{k_C^1 e^{3a_C^1(V-\Psi_s(1))}}{m_C^1 e^{-3b_C^1(V-\Psi_s(1))} + k_C^1 e^{3a_C^1(V-\Psi_s(1))}} \leq 1 \leq \tilde{C}.$$

Thanks to the monotonicity of C_s, it concludes the proof. $\qquad\square$

Remark 3.2. [Theorem 3.1](#) is worthy of interest if $\max\left(\tilde{K}_1, \tilde{K}_2\right) > 0$. This can be true if either $\beta_C^0(\widetilde{\Psi})\gamma_C^1(V - \widetilde{\Psi}) \geq \beta_C^1(V - \widetilde{\Psi})\gamma_C^0(\widetilde{\Psi})$ or $\varepsilon_C K \gamma_C^1(\Delta \Psi_1^{pzc}) \geq \beta_C^1(\Delta \Psi_1^{pzc})$, which is satisfied if

$$e^{3V} e^{-\widetilde{\Psi}} \geq \frac{m_C^0 m_C^1}{k_C^0 k_C^1} \quad \text{or} \quad e^{-3\Delta \Psi_1^{pzc}} \leq (\varepsilon_C K - 1) \frac{k_C^1}{m_C^1}.$$

Remark 3.3. We do not have any uniqueness result with our method. We can set partial results of uniqueness in the spirit of [Lemma 3.1](#). To guarantee the uniqueness of $(\Psi_s, \ell_s, \delta_s, C_s)$ one can impose for instance that F is strictly monotone, which adds new conditions on the parameters.

Remark 3.4. For $U = P, N$, there exists a unique solution to [(25)](#), given by formula [(31a)](#) and [(31b)](#). It is possible to impose conditions such that $\hat{J}_P$ and $\hat{J}_N$ are nonpositive fluxes or to ensure that P_s and N_s are non negative densities.

Remark 3.5. For the simplified model (**TM**), equations [(22)](#) and [(24a)](#) imply that both interfaces of the domain, in the pseudo-stationary case, move at a constant velocity. The velocity is prescribed by the solution to [(22)](#) and is clearly finite.

4. Numerical analysis of the simplified model

4.1. Presentation of the numerical scheme

The numerical scheme defined for toy model (**TM**) is the adaptation of the scheme (**S**) introduced in Section [2.2](#) to this simplified model. We denote it (**S-TM**).

*Numerical scheme (**S-TM**)*
The unknowns of the scheme are the discrete densities $(C_i)_{0 \leq i \leq I+1}$ and the discrete electric potential $(\Psi_i)_{0 \leq i \leq I+1}$, the velocity of the interfaces δ^h and the thickness of the domain ℓ^h.

- Scheme for Ψ:

$$-\frac{\lambda^2}{\ell^{h2}}(d\Psi_{i+\frac{1}{2}} - d\Psi_{i-\frac{1}{2}}) = 0, \quad 1 \leq i \leq I, \tag{33a}$$

$$\text{with } d\Psi_{i+\frac{1}{2}} = \frac{\Psi_{i+1} - \Psi_i}{h_{i+\frac{1}{2}}}, \quad 0 \leq i \leq I, \tag{33b}$$

$$\Psi_0 - \frac{\alpha_0}{\ell^h}d\Psi_{\frac{1}{2}} = \Delta\Psi_0^{pzc}, \tag{33c}$$

$$\Psi_{I+1} + \frac{\alpha_1}{\ell^h}d\Psi_{I+\frac{1}{2}} = V - \Delta\Psi_1^{pzc}. \tag{33d}$$

- Scheme for C:

$$\mathcal{G}_{C,i+\frac{1}{2}} - \mathcal{G}_{C,i-\frac{1}{2}} = 0, \quad 0 \leq i \leq I, \tag{34a}$$

$$\mathcal{G}_{C,i+\frac{1}{2}} = \frac{1}{h_{i+\frac{1}{2}}}\left(B\left(h_{i+\frac{1}{2}}\left(z_C d\Psi_{i+\frac{1}{2}} + \varepsilon_C \ell^h \delta^h\right)\right)C_i \right. \tag{34b}$$

$$\left. - B\left(-h_{i+\frac{1}{2}}\left(z_C d\Psi_{i+\frac{1}{2}} + \varepsilon_C \ell^h \delta^h\right)\right)C_{i+1}\right), \quad 1 \leq i \leq I, \tag{34c}$$

$$-\mathcal{G}_{C,\frac{1}{2}} = \ell^h r_C^0(C_0, \Psi_0), \tag{34d}$$

$$\mathcal{G}_{C,I+\frac{1}{2}} = \ell^h r_C^1(C_{I+1}, \Psi_{I+1}, V), \tag{34e}$$

where B is the Bernoulli function (19).

- Scheme for δ and ℓ:

$$\delta^h = \frac{k_d^0}{\Pi} e^{-5a_d^0 \Psi_0}, \tag{35a}$$

$$\ell^h = -K \frac{\mathcal{G}_{C,I+\frac{1}{2}}}{\delta^h}. \tag{35b}$$

In the next section, we show that the schemes (**S-TM**) is exact. It means that the exact solution to (**S-TM**) is a solution to the scheme. It is a well-known property of the Scharfetter–Gummel scheme for a stationary drift–diffusion equation when the drift velocity is the gradient of a potential (see for instance [17]). The novelty here is that the drift–diffusion equation is coupled with equations on the interface velocity δ and the size of the layer ℓ. However, we prove that the preservation of the steady-state by the Scharfetter–Gummel scheme still holds.

4.2. Existence of a solution for (*S-TM*)

Theorem 4.1. *Assume*

$$\min\left(\tilde{K}_1, \tilde{K}_2\right) < k_d^0 < \max\left(\tilde{K}_1, \tilde{K}_2\right),$$

where $\tilde{K}_1, \tilde{K}_2$ are defined in Theorem 3.1. *Then the scheme* (**S-TM**) *has a solution* $\left(\Psi^h, C^h, \delta^h, \ell^h\right) \in \left(\mathbb{R}^{I+2}\right)^2 \times \left(\mathbb{R}_+^*\right)^2$. *Moreover, there exists* $(\Psi_s, C_s, \delta_s, \ell_s)$ *solution to* (**TM**), *such that:*

$$\forall i \in [0, I+1], \quad \left(\Psi_i^h, C_i^h, \delta^h, \ell^h\right) = \left(\Psi_s(ih), C_s(ih), \delta_s, \ell_s\right). \tag{36}$$

Proof. *Existence.* Let $(\Psi_s, C_s, \delta_s, \ell_s)$ be a solution of (**TM**). Since (33) is exact on the linear solutions of (22), we define $\Psi_i^h = \Psi(ih), i \in [0, I+1]$ solution of (33) with $\ell^h = \ell_s$. We then fix

$$\delta^h = \delta_s = \frac{k_d^0}{\Pi} e^{-5a_d^0 \Psi_0^h}.$$

We observe that $\left(z_C d\Psi_{i+\frac{1}{2}} + \varepsilon_C \ell^h \delta^h\right)$ is constant, therefore the Scharfetter–Gummel scheme (34) is exact on (23). Define $\left(C_i^h\right) = (C(ih)), i \in [0, I+1]$, it is solution of (34). Finally (24b) implies (35b). It concludes the proof of the existence of a solution.

Any solution is exact. Let $\left(\Psi^h, C^h, \delta^h, \ell^h\right)$ be a solution of (**S-TM**). We apply Lemma 3.1 with $\ell = \ell^h$ it gives $(\Psi_{\ell^h}, C_{\ell^h}, \delta_{\ell^h}) \in (C^\infty[0,1])^2 \times \mathbb{R}_+^*$ a solution of (22)–(23)–(24a). Since Ψ_{ℓ^h} is linear and the scheme given by (33) is exact on linear function we have for all $i \in [0, I+1]$ $\Psi_i^h = \Psi_{\ell^h}(ih)$. Therefore (35a) implies $\delta^h = \delta_{\ell^h}$. The exactness of the Scharfetter–Gummel scheme gives $C_i^h = C_{\ell^h}(ih)$, for all $i \in [0, I+1]$. Then equations (34e) and (23c) implies $\mathcal{G}_{C^h, I+\frac{1}{2}} = \hat{J}_{C_{\ell^h}}$. Combined to (35b) we deduce that

$$\ell^h = -K \frac{\mathcal{G}_{C^h, I+\frac{1}{2}}}{\delta^h} = -K \frac{\hat{J}_{C_{\ell^h}}}{\delta_{\ell^h}}.$$

It shows that $(\Psi_{\ell^h}, C_{\ell^h}, \delta_{\ell^h}, \ell^h)$ is a solution to (**TM**) and concludes the proof.

Table A.1
Physical parameters of the test case.

D_1 (m$^2 \cdot$ s^{-1})	D_2 (m$^2 \cdot$ s^{-1})	D_3 (m$^2 \cdot$ s^{-1})
10^{-20}	10^{-6}	10^{-20}
m	Ω_{ox} (m$^3 \cdot$ mol)	Ω_{Fe} (m$^3 \cdot$ mol)
3	$4.474 \cdot 10^{-5}$	$7.105 \cdot 10^{-6}$
$\left(a_u^0, b_u^0\right)$ $(u = P, N, C, r)$	$\left(a_u^1, b_u^1\right)$ $(u = P, C)$	a_d^0
$(0.5, 0.5)$	$(0.5, 0.5)$	0

Table A.2
Scaled parameters of the test case.

$\Delta\Psi_0^{pzc}$		$\Delta\Psi_1^{pzc}$		$k_{d,ref}^0$
$-8.22136 \cdot 10^{-12}$		0		$64.267 \cdot 10^{-\text{pH}}$
P^m		N_{metal}		ρ_{hl}
2		$2.48502 \cdot 10^{-1}$		-5
λ^2		α_0		α_1
$1.05432 \cdot 10^{-3}$		0.177083		$8.854 \cdot 10^{-2}$
m_P^0	k_P^0	m_P^1	k_P^1
0	10^8	10^8	10^{14}
m_N^0	k_N^0	m_N^1	k_N^1
0	$2.10740 \cdot 10^{-19}$	$2.68111 \cdot 10^1$	$2.68111 \cdot 10^1$
m_C^0	k_C^0	m_C^1	k_C^1
$1.78113 \cdot 10^{-13}$	$4.474 \cdot 10^{47}$	0	7.85325

Remark 4.1. The convergence of the scheme (**S-TM**) towards (**TM**) is a straightforward consequence of the exactness property. This exactness property, peculiar to the Scharfetter–Gummel fluxes, enhance the choice of these fluxes when building the scheme (**S**). □

Acknowledgements

Appendix. Parameters used for the numerical experiments

All the numerical simulations have been done with the set of parameters given in Tables A.1 and A.2. The scaling process and the physical values used to obtain the scaled values in Table A.2 are detailed in [10, Section 5].

References

[1] C. Bataillon, F. Bouchon, C. Chainais-Hillairet, C. Desgranges, E. Hoarau, F. Martin, M. Tupin, J. Talandier, Corrosion modelling of iron based alloy in nuclear waste repository, Electrochim. Acta 55 (15) (2010) 4451–4467.
[2] N. Pilling, R. Bedworth, The oxidation of metals at high temperatures, J. Inst. Met. 29 (1923) 529–591.
[3] C. Chainais-Hillairet, I. Lacroix-Violet, On the existence of solutions for a drift-diffusion system arising in corrosion modelling, Discrete Contin. Dyn. Syst. Ser. B 20 (1) (2015) 77–92.
[4] C. Chainais-Hillairet, I. Lacroix-Violet, The existence of solutions to a corrosion model, Appl. Math. Lett. 25 (11) (2012) 1784–1789.
[5] C. Bataillon, F. Bouchon, C. Chainais-Hillairet, J. Fuhrmann, E. Hoarau, R. Touzani, Numerical methods for simulation of a corrosion model with moving numerical methods for simulation of a corrosion model with moving oxide layer, J. Comput. Phys. 231 (18) (2012) 6213–6231.
[6] C. Chainais-Hillairet, P.-L. Colin, I. Lacroix-Violet, Convergence of a Finite Volume Scheme for a Corrosion Model, Int. J. Finite Vol. 12 (2015).

C. Chainais-Hillairet, T.O. Gallouët / Nonlinear Analysis: Real World Applications 31 (2016) 38–56

[7] T. Aiki, A. Muntean, Existence and uniqueness of solutions to a mathematical model predicting service life of concrete structures, Adv. Math. Sci. Appl. 19 (1) (2009) 109–129.

[8] T. Aiki, A. Muntean, On uniqueness of a weak solution of one-dimensional concrete carbonation problem, Discrete Contin. Dyn. Syst. 29 (4) (2011) 1345–1365.

[9] T. Aiki, A. Muntean, A free-boundary problem for concrete carbonation: front nucleation and rigorous justification of the $\sqrt{t}$-law of propagation, Interfaces Free Bound. 15 (2) (2013) 167–180.

[10] C. Chainais-Hillairet, C. Bataillon, Mathematical and numerical study of a corrosion model, Numer. Math. 110 (1) (2008) 1–25.

[11] A.M. Il'in, A difference scheme for a differential equation with a small parameter multiplying the highest derivative, Mat. Zametki 6 (1969) 237–248.

[12] D. Scharfetter, H. Gummel, Large-signal analysis of a silicon read diode oscillator, IEEE Trans. Electron Devices 16 (1) (1969) 64–77.

[13] R.D. Lazarov, I.D. Mishev, P.S. Vassilevski, Finite volume methods for convection–diffusion problems, SIAM J. Numer. Anal. 33 (1) (1996) 31–55.

[14] H. Gajewski, K. Gärtner, On the discretization of van Roosbroeck's equations with magnetic field, Z. Angew. Math. Mech. 76 (5) (1996) 247–264.

[15] M. Chatard, Asymptotic behavior of the Scharfetter-Gummel scheme for the drift-diffusion model, in: Finite Volumes For Complex Applications. VI. Problems & Perspectives. Vol. 1, 2, in: Springer Proc. Math., vol. 4, Springer, Heidelberg, 2011, pp. 235–243.

[16] P.A. Markowich, C.A. Ringhofer, C. Schmeiser, Semiconductor Equations, Springer-Verlag, Vienna, 1990.

[17] C. Chainais-Hillairet, J. Droniou, Finite-volume schemes for noncoercive elliptic problems with Neumann boundary conditions, IMA J. Numer. Anal. 31 (1) (2011) 61–85.